Ultra-long pure longitudinal magnetization needle induced by annular vortex binary optics

Sicong Wang,[1,2] Xiangping Li,[1] Jianying Zhou,[2] and Min Gu[1,*]

[1] *Centre for Micro-Photonics, Faculty of Science, Engineering and Technology, Swinburne University of Technology, Hawthorn VIC 3122, Australia*

[2] *State Key Laboratory of Optoelectronic Materials and Technologies, Sun Yat-sen University, Guangzhou 510275, China*

**Corresponding author: mgu@swin.edu.au*

Received Month X, XXXX; revised Month X, XXXX; accepted Month X, XXXX; posted Month X, XXXX (Doc. ID XXXXX); published Month X, XXXX

In this Letter based on the Richards and Wolf diffraction theory an ultra-long optical needle with pure transverse polarization is numerically generated by tightly focusing an azimuthally polarized beam through an annular vortex binary filter. Such an ultra-long transversely polarized optical needle is generated through the π phase shift between adjacent rings of the binary filter. We show that such a pure transverse optical needle can induce pure longitudinal magnetization with a sub-wavelength lateral size (0.38λ) and an ultra-long longitudinal depth (7.48λ) through the inverse Faraday effect. The corresponding needle aspect ratio of 20 is twice as large as that of the longitudinal magnetization needle generated by electron beam lithography.

OCIS Codes: (210.3820) Magneto-optical materials; (260.5430) Polarization; (050.1380) Binary optics.

http://dx.doi.org/10.1364/OL.99.099999

As one of the two most fundamental aspects of electromagnetic phenomena, the manipulation of the magnetization in materials has attracted intensive research interests for appealing applications in data storage, spin wave operations and ferromagnetic semiconductor devices [1-3]. In particular, the generation of needle-like probes with pure longitudinal magnetization at a sub-wavelength scale is highly desired for ultra-high density magnetic storage as well as fabricating magnetic lattices for spin wave operation and atomic trapping [1,2,4-7]. Even though electron beam lithography has enabled the fabrication of such sub-wavelength structures with longitudinal magnetization and the aspect ratio of them can be up to 9.3 [1], the associated high cost and complicated near-field processes limit their practical applications.

On the other hand, light-induced magnetization through the inverse Faraday effect (IFE) [8-14] has been conceived as an invasive and far-field method to realize a longitudinal magnetization probe. As such, tightly focusing a circularly polarized beam with a high numerical aperture (NA) objective has been demonstrated to be an essential method for confining light-induced longitudinal magnetization in a diffraction-limited region [15]. Moreover, the incorporation of the amplitude modulation or binary optics (the $0/\pi$ phase modulation) offers a tremendous flexibility to elongate focal fields in the propagating direction to form optical needles [16-21]. The implementation of these modulations on a circularly polarized beam can lead to a sub-wavelength confined light-induced magnetization [15]; however, none of these approaches can realize ultra-long needle beams with pure longitudinal magnetization owing to the depolarization effect under the tightly focusing condition [22]. Even though the interaction between a phase singularity and a polarization singularity can lead to pure longitudinal magnetization through the IFE, the aspect ratio of the focal voxel is restricted to approximately 3 due to the lack of the capability to extend the constructive interference beyond 1.29λ in the propagating direction [23].

The combination of vortex [23-25], amplitude modulation [16-18,26] and binary optics [19-21] may provide a new way to manipulate the focal field distribution, and hence the light-induced magnetization through the IFE. In this Letter, an annular vortex binary filter is proposed to modulate the incident azimuthally polarized beam for generating an ultra-long needle-like beam with pure longitudinal magnetization. The annular vortex binary filter composed of spiral phase rings with a π shift between adjacent rings plays two roles. On the one hand, it can serve as the polarization convertor so that circular or elliptical polarization can be generated in the focal region. On the other hand, it can generate an elongated field distribution in the propagating direction for ultra-long optical needles by shrinking the lateral size and extending constructive interference in the propagating direction through the π phase shift between adjacent rings. In contrast to conventional optical needles with dominant longitudinally polarized fields [16-21], an optical needle with pure transverse polarization is formed. Since the light-induced magnetization through the IFE is proportional to the cross product between the focal electric field and its conjugate [9] such a pure transverse optical needle can induce pure longitudinal magnetization with a sub-wavelength lateral size of 0.38λ and an ultra-long longitudinal depth of 7.48λ, which corresponds to an aspect ratio of 20.

As shown in Fig. 1, an azimuthally polarized beam modulated by an annular vortex binary filter is focused on a nonabsorbing isotropic magneto-optical material by a high NA (0.95) aplanatic lens. Different from the traditional binary optics with $0/\pi$ phase modulation, a vortex binary filter with a phase difference of π between adjacent spiral phase rings is introduced. The helicities of

the vortex rings remain the same. It is worth noting that the configuration of directions of the helicity of the annular vortex binary filters can be variable depending on the applications. R_a and R_p marked on filter 1 are adjustable parameters to optimize the field distribution. The fixed parameter R_0 is the radius of the filter and the lens. Filter 1 and filter 2 correspond to the topological charges m=+1 and m=-1, respectively. Filter 1 can induce the magnetization with the same orientation as the propagating direction of the beam, while filter 2 with the opposite helicity can induce the magnetization with the opposite orientation. An obstruction disc with a radius of R_a is utilized in the filters.

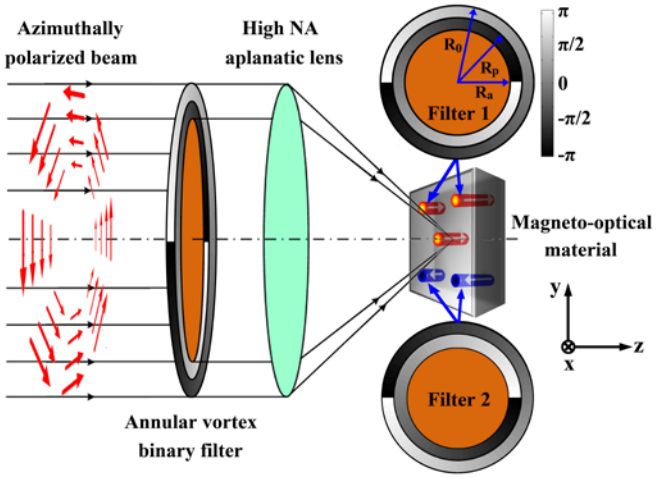

Fig. 1. Schematic illustration of the set-up to generate the pure longitudinal magnetization needle. By using filter 1 at the back aperture of the objective, magnetization with the same orientation as the propagating direction of the beam (red "bars") can be induced. Magnetization with the opposite orientation (blue "bars") can be induced by using filter 2.

The incident beam through the filter at the back aperture of the objective can be expressed as

$$\mathbf{E}_{inc} = E_0 T_\phi \mathbf{e}_\phi = -\frac{i}{\sqrt{2}} E_0 T_\phi (e^{-i\phi}\mathbf{e}_L - e^{i\phi}\mathbf{e}_R), \quad (1)$$

where

$$T_\phi = \begin{cases} e^{i(m\phi+\pi)} & R_a \le r \le R_p \\ e^{im\phi} & R_p < r \le R_0 \end{cases}. \quad (2)$$

The filter is illuminated by a plane wave and hence E_0=1. r and ϕ are the polar coordinates in the incident space. $\mathbf{e}_\phi$, $\mathbf{e}_L$ and $\mathbf{e}_R$ are the unit base vectors of azimuthal, left-handed and right-handed circular polarizations, respectively. Equations (1) and (2) indicate that whenever m=+1 or m=-1, one of the circular polarization components loses its phase singularity and hence forms a plane phase front. Thus, it results in circular polarization at the center of the focal field. Similar situations occur in the focused Laguerre Gaussian vortex beams [25].

According to the Richards and Wolf diffraction theory [27], the electric field distribution in the focal region can be expressed as

$$\mathbf{E}(r,\varphi,z) = \begin{bmatrix} \mathbf{E}_r \\ \mathbf{E}_\varphi \\ \mathbf{E}_z \end{bmatrix} = Ai^m \int_{\theta_a}^{\theta_0} T_\varphi \begin{bmatrix} V_1 \\ iV_2 \\ 0 \end{bmatrix} e^{ikz\cos\theta} \sqrt{\cos\theta}\sin\theta d\theta, \quad (3)$$

where

$$V_1 = J_{m-1}(kr\sin\theta) + J_{m+1}(kr\sin\theta), \quad (4)$$

$$V_2 = J_{m-1}(kr\sin\theta) - J_{m+1}(kr\sin\theta), \quad (5)$$

and

$$T_\varphi = \begin{cases} e^{i(m\varphi+\pi)} & \theta_a \le \theta \le \theta_p \\ e^{im\varphi} & \theta_p < \theta \le \theta_0 \end{cases}. \quad (6)$$

Here A is a constant. r, φ and z are the cylindrical coordinates in the focal space. J_0 and J_2 denote Bessel functions of the first kind. θ_a, θ_p and θ_0 are the converging angles corresponding to the radial positions R_a, R_p and R_0, respectively. Equation (3) is represented in cylindrical vectorial components and it indicates that the filter transforms a beam with pure azimuthal polarization into a beam with radial and azimuthal polarization components which are essential to obtain longitudinal magnetization at the focus.

According to the energy considerations [9], the phenomenological expression of the IFE can be represented as

$$\mathbf{M} = i\gamma \mathbf{E}\times\mathbf{E}^*, \quad (7)$$

where $\mathbf{E}$ is the electric field, $\mathbf{E}^*$ is its conjugate, and γ is a real constant proportional to the susceptibility of the material [9-11]. By substituting Eqs. (3)-(6) into Eq. (7), the magnetization field can be given by

$$\mathbf{M} = 2\gamma |A|^2 \,\mathrm{Re}(I_1 \cdot I_2)\mathbf{e}_z, \quad (8)$$

where

$$I_1 = \int_{\theta_a}^{\theta_0} T_\varphi V_1 e^{ikz\cos\theta}\sqrt{\cos\theta}\sin\theta d\theta, \quad (9)$$

and

$$I_2 = \int_{\theta_a}^{\theta_0} T_\varphi^* V_2 e^{-ikz\cos\theta}\sqrt{\cos\theta}\sin\theta d\theta. \quad (10)$$

$\mathbf{e}_z$ is the unit base vector in the longitudinal (z) direction. Equation (8) indicates that the light-induced magnetization is pure longitudinal.

Reducing the light spot size by increasing R_a is often accompanied by strong side lobes, which can degrade the resolution [28, 29]. To avoid the influence by the strong side lobes, R_a is optimized with a balance between the elongation of the focal field and the peak values of the lateral side lobes no larger than 0.35 of that of the principal lobe. Hence R_a=0.9R_0 and the corresponding R_p = 0.9192R_0 are chosen.

Figure 2 shows the electric field distribution in the focal plane. The topological charge m=1 (filter 1). Figure 2(a) illustrates the phase distributions of E_r and E_φ. The constant A is not considered. The cross-sections of the normalized amplitudes of E_r and E_φ are shown in Fig. 2(b). Compared with E_r the phase of E_φ is delayed by π/2. In the

area $r<0.32\lambda$, E_r and E_φ have the same sign, which means that left-handed circular or elliptical polarization is obtained in this area as depicted in Fig. 2(c) and thus can induce magnetization with +z orientation. In the area $0.32\lambda<r<0.66\lambda$, E_r and E_φ are with opposite signs and the magnetization orientation can be reversed owing to the right-handed circular or elliptical polarization obtained in this area. The magnetization strength is zero at $r=0.32\lambda$ and 0.66λ because the radial and azimulthal components are incapable of inducing magnetization via the IFE.

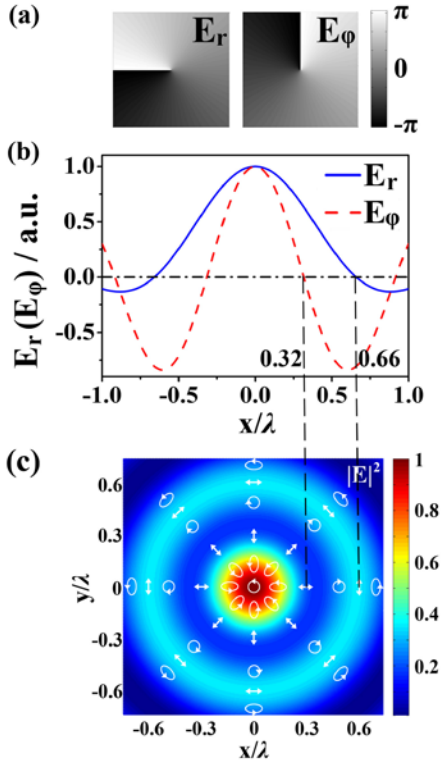

Fig. 2. Electric field distribution in the focal plane (m=1). (a) The phase distributions of E_r and E_φ. (b) The cross-sections of the normalized amplitudes of E_r and E_φ. (c) The electric energy density and polarization distributions. λ is the wavelength of the incident beam in vacuum.

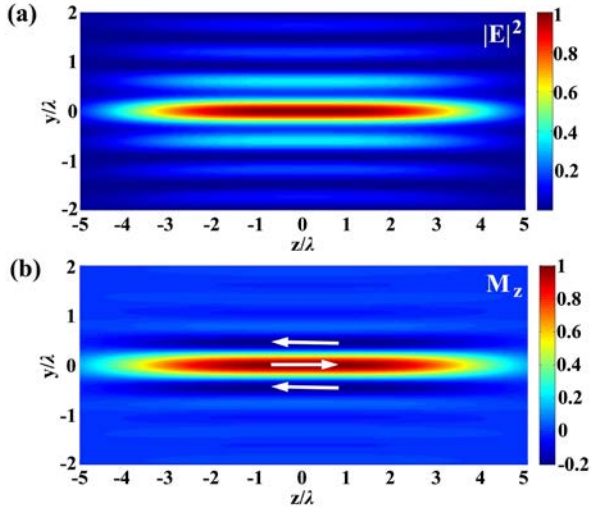

Fig. 3. Normalized electric energy density distribution (a) and magnetization distribution (b) in the axial plane.

Owing to the elongation effect of field distributions by the binary filter, an optical needle with pure transverse polarization is formed as shown in Fig. 3(a). Attributed to this pure transverse optical needle, the field distribution does not change remarkably within a wide range beyond the focal plane in the z direction, and thus magnetization distribution should not significantly vary, namely a pure longitudinal magnetization needle, is induced by the pure transversely polarized optical needle as shown in Fig. 3(b).

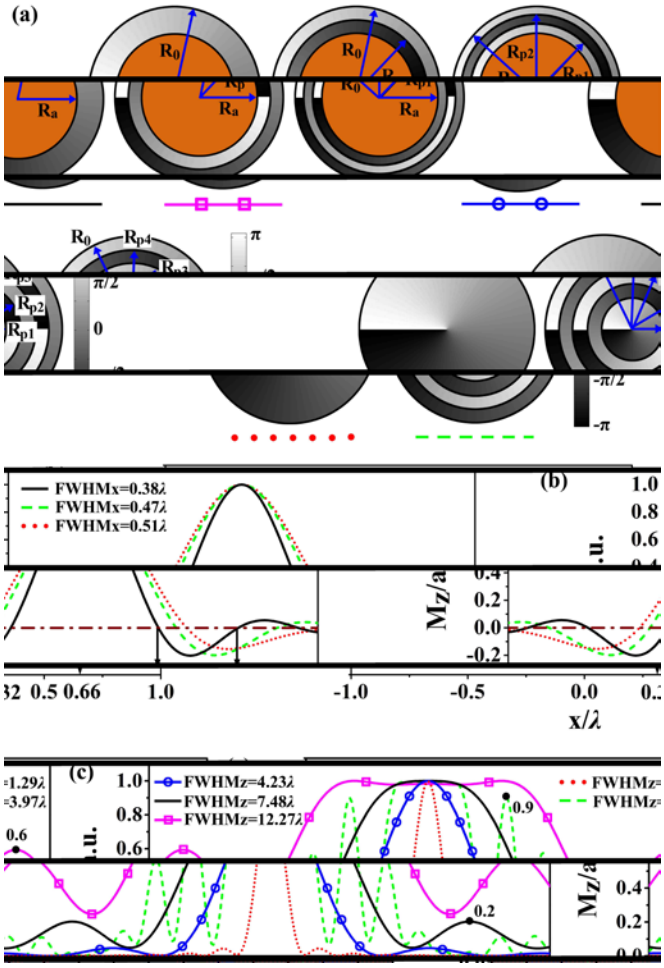

Fig. 4. Magnetization distributions with different modulations on the incident beam. (a) Different vortex filters. (b) Cross-sections (along x axis) of the normalized magnetization distributions in the focal plane. (c) Cross-sections (along z axis) of the normalized magnetization distributions. The lines with different colors and styles under the filters in (a) represent the corresponding lateral and longitudinal cross-sections of the induced magnetization in (b) and (c).

The double-ring annular vortex binary filter can generate ultra-long focal depth without significant axial side lobes. Figure 4 depicts the comparison of magnetization distributions by different modulations on the incident beam. The magnetization fields modulated by the single-ring ($R_a=0.9R_0$), aforementioned double-ring and triple-ring ($R_a=0.9R_0$, $R_{p1}=0.9098R_0$, and $R_{p2}=0.9396R_0$) annular vortex binary filters have almost the same lateral sizes, and the full widths at half maximum (FWHM) are about 0.38λ. All of them are much

smaller than that with vortex phase plate modulation only (0.51λ). With the amplitude obstruction disc, the longitudinal depth of the magnetization field is elongated by more than three times. The double-ring vortex binary filter can further extend the long depth to 7.48λ, and the peak of the axial side lobe is only 20% of the maximum of the principal lobe. In the triple-ring case, a longer depth of 12.27λ is obtained, but much higher side lobes with a peak value around 60% of the principal lobe peak value accompanies as shown in Fig. 4(c). It can be expected that using more rings can extend the needle length but with degraded qualities accompanying significant axial side lobes.

A generally used pure vortex binary filter with five rings which was used to generate longitudinally polarized optical needles [19,20] can only enable a magnetization needle with a lateral size of 0.47λ and a length of 3.97λ. The incident beam is the Bessel-Gaussian beam with the same parameters mentioned in Ref. [19]. In this case $R_{p1}=0.337R_0$, $R_{p2}=0.5701R_0$, $R_{p3}=0.9273R_0$, and $R_{p4}=0.9823R_0$. Even though a higher optical efficiency can be obtained, it is ruled out for consideration in this application as strong axial side lobes appear with an intensity of nearly 90% of the principal lobe peak value.

In conclusion, an ultra-long needle beam with pure longitudinal magnetization is numerically generated through tightly focusing an azimuthally polarized beam by an annular vortex binary filter. A pure transversely polarized optical needle can be generated in the focal region by the annular vortex binary filter. Through the IFE, a pure longitudinal magnetization needle with a sub-wavelength lateral size and an aspect ratio of 20 is realized. The demonstrated pure longitudinal magnetization needle with a high aspect ratio holds great potentials in ultrahigh density all-optical magnetic recording and fabricating magnetic lattices for spin wave operation and atomic trapping with flexibility.

This work is supported by the Australian Research Council (ARC) Laureate Fellowship scheme (FL100100099). Mr. Sicong Wang acknowledges the financial support from the China Scholarship Council (grant No. [2013] 3009) and the National Basic Research Program of China (2012CB921904) for his study in Australia.

References

1. S. Y. Chou, M. S. Wei, P. R. Krauss, and P. B. Fischer, J. Appl. Phys. **76**, 6673 (1994).
2. S. A. Nikitov, Ph. Tailhades, C. S. Tsai, J. Magn. Magn. Mater. **236**, 320 (2001).
3. D. Chiba, M. Sawicki, Y. Nishitani, Y. Nakatani, F. Matsukura, and H. Ohno, Nature **455**, 515 (2008).
4. I. L. Lyubchanskii, N. N. Dadoenkova, M. I. Lyubchanskii, E. A. Shapovalov, and Th. Rasing, J. Phys. D: Appl. Phys. **36**, R277 (2003).
5. P. D. Ye, D. Weiss, R. R. Gerhardts, M. Seeger, K. von Klitzing, K. Eberl, and H. Nickel, Phys. Rev. Lett. **74**, 3013 (1995).
6. M. –O. Mewes, M. R. Andrews, N. J. van Druten, D. M. Kurn, D. S. Durfee, and W. Ketterle, Phys. Rev. Lett. **77**, 416 (1996).
7. C. V. Saba, P. A. Barton, M. G. Boshier, I. G. Hughes, P. Rosenbusch, B. E. Sauer, and E. A. Hinds, Phys. Rev. Lett. **82**, 468 (1999).
8. L. P. Pitaevskii, Sov. Phys. JETP-USSR **12**, 1008 (1961).
9. P. S. Pershan, Phys. Rev. **130**, 919 (1963).
10. J. P. van der Ziel, P. S. Pershan, and L. D. Malmstrom, Phys. Rev. Lett. **15**, 190 (1965).
11. P. S. Pershan, J. P. van der Ziel, and L. D. Malmstrom, Phys. Rev. **143**, 574 (1966).
12. A. V. Kimel, A. Kirilyuk, P. A. Usachev, R. V. Pisarev, A. M. Balbashov, and Th. Rasing, Nature **435**, 655 (2005).
13. C. D. Stanciu, F. Hansteen, A. V. Kimel, A. Kirilyuk, A. Tsukamoto, A. Itoh, and Th. Rasing, Phys. Rev. Lett. **99**, 047601 (2007).
14. A. V. Kimel, A. Kirilyuk, and Th. Rasing, Laser & Photon. Rev. **1**, 275 (2007).
15. Y. J. Zhang, Y. Okuno, and X. Xu, J. Opt. Soc. Am. B **26**, 1379 (2009).
16. K. Kitamura, K. Sakai, and S. Noda, Opt. Express **18**, 4518 (2010).
17. J. Lin, K. Yin, Y. Li, and J. Tan, Opt. Lett. **36**, 1185 (2011).
18. H. Dehez, A. April, and M. Piche, Opt. Express **20**, 14891 (2012).
19. H. Wang, L. Shi, B. Lukyanchuk, C. Sheppard, and C. T. Chong, Nat. Photon. **2**, 501 (2008).
20. K. Huang, P. Shi, X. Kang, X. Zhang, and Y. Li, Opt. Lett. **35**, 965 (2010).
21. J. Wang, W. Chen, and Q. Zhan, Opt. Express **18**, 21965 (2010).
22. M. Gu, *Advanced Optical Imaging Theory* (Springer, 2000).
23. Y. Jiang, X. Li, and M. Gu, Opt. Lett. **38**, 2957 (2013).
24. D. Ganic, X. Gan, and M. Gu, Opt. Express **11**, 2747 (2003).
25. K. Kitamura, K. Sakai, N. Takayama, M. Nishimoto, and S. Noda, Opt. Lett. **37**, 2421 (2012).
26. X. Li, T. H. Lan, C. H. Tien, and M. Gu, Nat. Commun. **3**, 998 (2012).
27. B. Richards and E. Wolf, Proc. Roy. Soc. A **253**, 358-379 (1959).
28. G. M. Lerman and U. Levy, Opt. Express **16**, 4567 (2008).
29. X. Hao, C. Kuang, T. Wang, and X. Liu, Opt. Lett. **35**, 3928 (2010).

References

1. S. Y. Chou, M. S. Wei, P. R. Krauss, and P. B. Fischer, "Single domain magnetic pillar array of 35 nm diameter and 65 Gbits/in.2 density for ultrahigh density quantum magnetic storage," J. Appl. Phys. **76**, 6673 (1994).
2. S. A. Nikitov, Ph. Tailhades, C. S. Tsai, "Spin waves in periodic magnetic structures-magnonic crystals," J. Magn. Magn. Mater. **236**, 320 (2001).
3. D. Chiba, M. Sawicki, Y. Nishitani, Y. Nakatani, F. Matsukura, and H. Ohno, "Magnetization vector manipulation by electric fields," Nature **455**, 515 (2008).
4. I. L. Lyubchanskii, N. N. Dadoenkova, M. I. Lyubchanskii, E. A. Shapovalov, and Th. Rasing, "Magnetic photonic crystals," J. Phys. D: Appl. Phys. **36**, R277 (2003).
5. P. D. Ye, D. Weiss, R. R. Gerhardts, M. Seeger, K. von Klitzing, K. Eberl, and H. Nickel, "Electrons in a Periodic Magnetic Field Induced by a Regular Array of Micromagnets," Phys. Rev. Lett. **74**, 3013 (1995).
6. M. –O. Mewes, M. R. Andrews, N. J. van Druten, D. M. Kurn, D. S. Durfee, and W. Ketterle, "Bose-Einstein Condensation in a Tightly Confining dc Magnetic Trap," Phys. Rev. Lett. **77**, 416 (1996).
7. C. V. Saba, P. A. Barton, M. G. Boshier, I. G. Hughes, P. Rosenbusch, B. E. Sauer, and E. A. Hinds, "Reconstruction of a Cold Atom Cloud by Magnetic Focusing," Phys. Rev. Lett. **82**, 468 (1999).
8. L. P. Pitaevskii, "Electric forces in a transparent dispersive medium," Sov. Phys. JETP-USSR **12**, 1008 (1961).
9. P. S. Pershan, "Nonlinear Optical Properties of Solids: Energy considerations," Phys. Rev. **130**, 919 (1963).
10. J. P. van der Ziel, P. S. Pershan, and L. D. Malmstrom, "Optically-induced magnetization resulting from the inverse Faraday effect," Phys. Rev. Lett. **15**, 190 (1965).
11. P. S. Pershan, J. P. van der Ziel, and L. D. Malmstrom, "Theoretical Discussion of the Inverse Faraday Effect, Raman Scattering, and Related Phenomena," Phys. Rev. **143**, 574 (1966).
12. A. V. Kimel, A. Kirilyuk, P. A. Usachev, R. V. Pisarev, A. M. Balbashov, and Th. Rasing, "Ultrafast non-thermal control of magnetization by instantaneous photomagnetic pulses," Nature **435**, 655 (2005).
13. C. D. Stanciu, F. Hansteen, A. V. Kimel, A. Kirilyuk, A. Tsukamoto, A. Itoh, and Th. Rasing, "All-Optical Magnetic Recording with Circularly Polarized Light," Phys. Rev. Lett. **99**, 047601 (2007).
14. A. V. Kimel, A. Kirilyuk, and Th. Rasing, "Femtosecond opto-magnetism: ultrafast laser manipulation of magnetic materials," Laser & Photon. Rev. **1**, 275 (2007).
15. Y. J. Zhang, Y. Okuno, and X. Xu, "All-optical magnetic superresolution with binary pupil filters," J. Opt. Soc. Am. B **26**, 1379 (2009).
16. K. Kitamura, K. Sakai, and S. Noda, "Sub-wavelength focal spot with long depth of focus generated by radially polarized narrow-width annular beam," Opt. Express **18**, 4518 (2010).
17. J. Lin, K. Yin, Y. Li, and J. Tan, "Achievement of longitudinally polarized focusing with long focal depth by amplitude modulation," Opt. Lett. **36**, 1185 (2011).
18. H. Dehez, A. April, and M. Piche, "Needles of longitudinally polarized light: guidelines for minimum spot size and tunable axial extent," Opt. Express **20**, 14891 (2012).
19. H. Wang, L. Shi, B. Lukyanchuk, C. Sheppard, and C. T. Chong, "Creation of a needle of longitudinally polarized light in vacuum using binary optics," Nat. Photon. **2**, 501 (2008).
20. K. Huang, P. Shi, X. Kang, X. Zhang, and Y. Li, "Design of DOE for generating a needle of a strong longitudinally polarized field," Opt. Lett. **35**, 965 (2010).
21. J. Wang, W. Chen, and Q. Zhan, "Engineering of high purity ultra-long optical needle field through reversing the electric dipole array radiation," Opt. Express **18**, 21965 (2010).
22. M. Gu, *Advanced Optical Imaging Theory* (Springer, 2000).
23. Y. Jiang, X. Li, and M. Gu, "Generation of sub-diffraction-limited pure longitudinal magnetization by the inverse Faraday effect by tightly focusing an azimuthally polarized vortex beam," Opt. Lett. **38**, 2957 (2013).
24. D. Ganic, X. Gan, and M. Gu, "Focusing of doughnut laser beams by a high numerical-aperture objective in free space," Opt. Express **11**, 2747 (2003).
25. K. Kitamura, K. Sakai, N. Takayama, M. Nishimoto, and S. Noda, "Focusing properties of vector vortex beams emitted by photonic-crystal lasers," Opt. Lett. **37**, 2421 (2012).
26. X. Li, T. H. Lan, C. H. Tien, and M. Gu, "Three-dimensional orientation-unlimited polarization encryption by a single optically configured vectorial beam," Nat. Commun. **3**, 998 (2012).
27. B. Richards and E. Wolf, "Electromagnetic diffraction in optical systems II. Structure of the image field in an aplanatic system," Proc. Roy. Soc. A **253**, 358-379 (1959).
28. G. M. Lerman and U. Levy, "Effect of radial polarization and apodization on spot size under tight focusing conditions," Opt. Express **16**, 4567 (2008).
29. X. Hao, C. Kuang, T. Wang, and X. Liu, "Phase encoding for sharper focus of the azimuthally polarized beam," Opt. Lett. **35**, 3928 (2010).